

Application of hydrochemical and isotopic techniques to understand groundwater recharge and flow systems in the Dawa River basin, southern Ethiopia

Fikadu Woldemariam^{1,2} · Tenalem Ayenew¹

Received: 29 August 2015 / Accepted: 25 May 2016 / Published online: 13 June 2016
© Springer-Verlag Berlin Heidelberg 2016

Abstract The study of groundwater recharge and of flow systems is crucial to understand availability and sustainability of groundwater resources. This study uses hierarchical cluster analysis (HCA) and various graphical plots of hydrochemical and isotopic data to examine groundwater recharge and the dynamics of flow system in the Dawa River basin. HCA has classified the water samples into five distinctive clusters. Clusters I, II, and III represent the volcanic and most parts of the basement terrain. These clusters are distinguished by low EC, high percentages of HCO_3^- and Ca^{2+} , Mg^{2+} , or Na^+ , and dominantly (Ca, Mg, Na, K)– HCO_3^- -type water. Cluster IV contains sulfate-type water with high percentage of $\text{Ca}^{2+} + \text{Mg}^{2+}$ and represents sedimentary terrain. Cluster V, characterized by high EC and abundant Na^+ and $\text{SO}_4^{2-} + \text{Cl}^-$, is sited at few locations along dry riverbeds. In the basement terrain, the chemical composition of groundwater varies greatly over short distances. In most parts of the basin, groundwater contains elevated levels of tritium at amount comparable to local rainfall. These chemical characteristics supported with tritium data indicate the dominance of groundwater of local flow systems, short residence time, and modern recharge in the basin. Stable isotope data indicate that in the semi-arid region, recharge occurs from high-intensity rainfall.

Difference in $\delta^{18}\text{O}$ and $\delta^2\text{H}$ between the northern and the southern and southeastern groundwater supports distinct recharge sources and the absence of regional groundwater flow between the two regions. Converging evidences reveal that the traditional regional groundwater flow model which is common in most large river basins of Ethiopia does not hold true in the Dawa River basin.

Keywords Dawa River basin · Groundwater flow system · Recharge · Cluster analysis · Isotopes

Introduction

Groundwater flows from recharge to discharge areas at local, intermediate, and/or regional scales whereby the scale of flow is determined by topography and hydraulic characteristics of underlying rocks (Tóth 1963; Bugliosi 1999). Understanding groundwater flow patterns is significant in locating groundwater of optimum quality (Toth 1984) and quantity (Furlong et al. 2011). Regional flow is important to supply lowland aquifers (Todd and Mays 2004; Kebede et al. 2007) and, therefore, valuable for the occurrence of good quantity groundwater particularly in semiarid and arid climatic areas where local recharge is believed to be scant (Bisson and Lehr 2004). Understanding aspects of groundwater recharge is also crucial for successful groundwater resources development and management program (Danskin 1998). Methods available to determine groundwater flow patterns include investigating groundwater levels and groundwater flow modeling (Zhou and Li 2011). Groundwater flow patterns and nature of groundwater recharge can also be characterized through study of hydrochemical pattern (Ophori and Toth 1989; Dalton and Upchurch 1978; Kebede et al. 2005) and environmental isotopes (Kebede 2013).

✉ Fikadu Woldemariam
fikaduwoldemariam@yahoo.com

Tenalem Ayenew
tenualem@gmail.com

¹ College of Natural and Computational Sciences, School of Earth Sciences, Addis Ababa University, POB 1176, Addis Ababa, Ethiopia

² College of Natural and Computational Sciences, Department of Geology, Dilla University, P.O.Box 419, Dilla, Ethiopia

The Dawa River basin of southern Ethiopia is characterized by complex geologic setting expressed by a diversified lithology and structural framework attributable to the basin's location in the region of multiple phases of volcanotectonic events (Woldehaimanot and Behrmann 1995; Worku and Schandemeier 1996; Hunegnaw et al. 1998). Typically, the basement complex is laterally emplaced in the middle parts of the basin between the highland volcanic rocks in the northwest and the lowland extensive sedimentary formation in the southeast. Owing to geological complexity, locating groundwater of good quantity and quality is the main concern of hydrogeological practitioners, particularly, in semiarid and arid regions of the river basin. There are only few previous hydrogeological studies available. Some of these studies such as Belete et al. (2000), MoWIE (2007), Zewdie and Nahusenay (2011), and Zewdie and Sima (2011) qualitatively classified rocks of the region into high, intermediate, and poor groundwater potential zones and provided preliminary information on the groundwater chemistry of the area. Other regional works, which includes the study area, provided broad understanding of how groundwater occurs in different lithologic terrains of Ethiopia (Kebede 2013) and basement rocks in particular (Deyassa et al. 2014). No detailed study is available dealing with groundwater recharge and flow systems in the basin. In particular, the effect that the basement complex in the center of the region poses on the scale of groundwater flow system of the river basin is not known. On the other hand, detailed hydraulic characteristics of particular rock and its spatial association with the other units are not known. It is also difficult to establish these hydrogeological parameters with the methods that depend on well data due to the limited and incomplete water-well information in the area. As a result, in the Dawa River basin, it is difficult to establish the nature of groundwater flow pattern using methods like flow modeling or based on existing groundwater levels.

The main objective of this investigation is to examine the nature of groundwater recharge and flow pattern in the basin. The study uses hierarchical cluster analysis (HCA) and various graphical plots of hydrochemical and isotopic data. The results of this study will add to the hydrogeological understanding of the area that helps in whether or not to consider the traditional regional groundwater flow model in the course of water well sitting and effective groundwater management activities in the basin.

Description of the study area

Location and physiography

The Dawa River basin is located in East Africa between 3.92°–6.47°N and 38.02°–42.08°E. It covers area of

58,961 km² in three countries: Ethiopia, Kenya, and Somalia. This study covers 81 % of total area of the basin that falls in Ethiopian territory (Fig. 1). The maximum and minimum elevation is 3089 and 169 m above sea level (masl) near the northwestern end of the basin and at the river outlet, respectively. The overall surface inclination of the basin is toward southeast. Much of the area in the northern and northwestern highland is characterized by ridges and associated gorges, while in the southwest, south-central, and southeast topography is characterized by leveled ground with scattered hills, low relief elongated valleys, and steep land adjacent to the main river (Fig. 1).

Climate

The northern, south-central, and southeastern parts of the study area are defined by humid, semiarid, and arid climatic condition, respectively (Gamachu 1977). Mean annual rainfall is about 1500 mm at the northern end, and it decreases alongside elevation to 200 mm near the river outlet. The rainfall exhibits bimodal seasonal pattern with maximum and minimum rainfall peak in May and October, respectively. The annual mean temperature is about 15.5 °C above 2000 masl and 28 °C below 500 masl.

Geology and hydrogeology

The basin is covered by Precambrian basement rocks, Mesozoic sedimentary formations, Tertiary volcanic rocks, and recent alluvial deposits. Precambrian basement rocks cover the central part of the basin. Its geological evolution is linked to East African Orogeny (Kroner and Stern 2004). According to Yibas et al. (2002), two different tectonostratigraphic terrains were identified—(1) granitoid gneiss, and (2) fold and thrust belts (Fig. 2). The former consist high-grade gneisses and granite intrusions and compositionally varying between acidic and basic, whereas the latter is N–S stripes of low-grade metamorphic rocks of dominantly basic composition.

Tertiary flood basalts and intercalated silicic volcanic rocks of Ethiopia (Mohr and Zanettin 1988) cover northwestern part of the study area (Fig. 2) overlying the basement rocks. Near the northern and northwestern end of the study area, 20–30 m thick unwelded tuffs and ignimbrite overlie the basaltic lava flows.

Jurassic to Cretaceous sedimentary formations cover southeastern part of the study area (Fig. 2). From bottom to top, stratigraphic sequence includes Adigrat Sandstone (white sand), Hamanlie Formation (dominantly limestone with minor gypsum intercalation), Urandab Formation (calcareous shale with minor gypsum and limestone), Gebradare Formation (dominantly marl with some limestone), and Gorrahe Formation (dominantly gypsum with subordinate limestone,

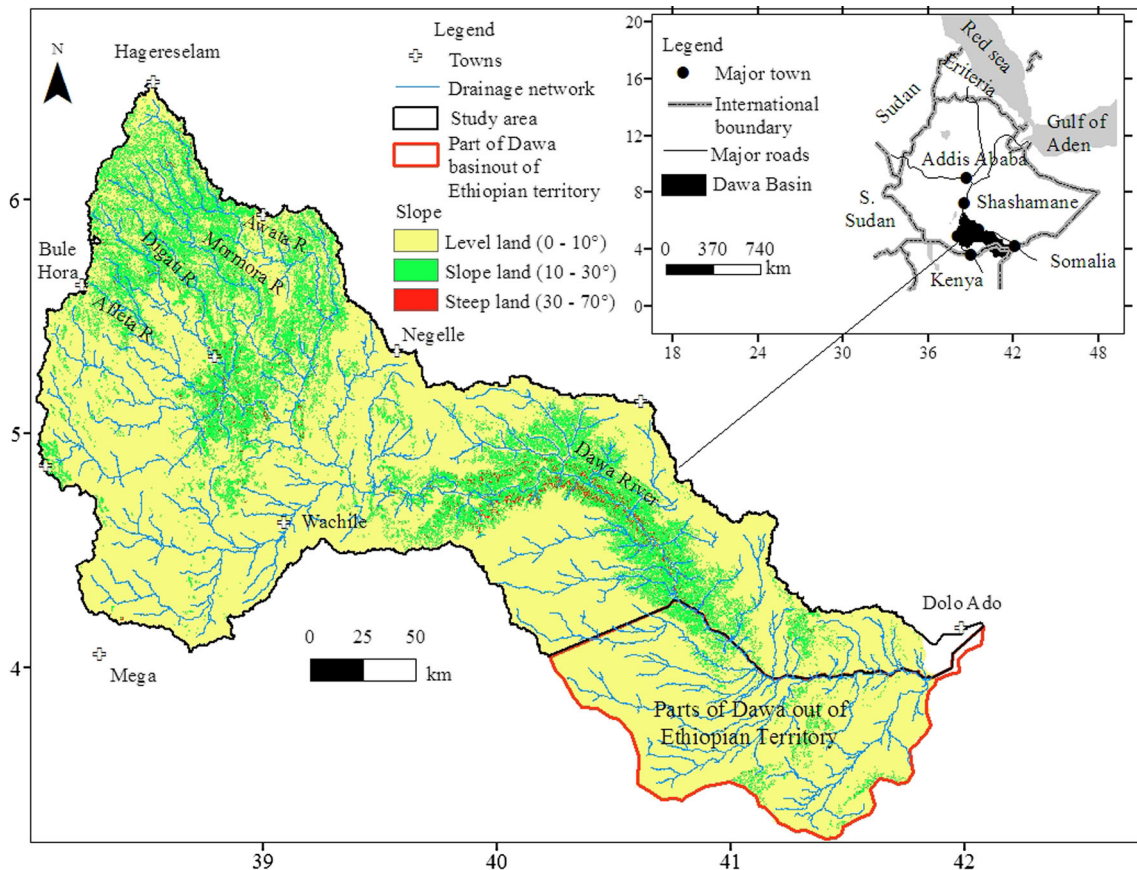


Fig. 1 Location, slope, and drainage map of study area

marl, and shale) (Assefa 1988). Overlying the basement rock thickness of the Mesozoic succession is about 5000 m near the southeast end of the study area (Hunegnaw et al. 1998). However, thinning in the northwest direction, it finally pinches out near 39.5° longitude. This suggests the general tilting and thickening of the whole sedimentary sequence takes place in a southeasterly direction.

Alluvial deposits are mainly composed of clay, silt, and sand and occur throughout the region. These sediments have accumulated in low-lying areas and along dry riverbeds (Fig. 2). Field exposure reveals that these sediments are up to 20-m-thick overlying gneissic bedrock.

As a result of multiple phases of tectonic activity, N–S, NW–SE, NE–SW, and E–W trending sets of fracture have affected rocks of the study area (Fig. 2). N–S and NE–SW fracture systems are largely occur in the fold and thrust belts and usually affected by the later on shearing/strike-slipping (Abdelsalam and Stern 1996; Worku 1996). NE–SW and E–W fractures cut and displace the N–S fractures (Hamrla 1977; Kozyrev et al. 1982). NW–SE trending fractures have dominantly affected the gneissic terrain and sedimentary sequences.

In general, the basaltic unit is characterized by the repeated occurrence of highly fractured and/or scoriaceous

basaltic layers at intervals of 10–20 m as observed in bore logs. As a result, basaltic rock is a highly porous and transmissive hydrostratigraphic unit in the region. In the tuffs and ignimbrites, fractures and joints are not traceable due to intense weathering that has produced thick clay soil. Existing water supply data suggest that groundwater occurrence and movement in the basement terrain of the study area is associated with the fracture network (Fig. 2). In general, fractures of the study area are short in length and are either not interconnected or cut by the short transverse fractures (Fig. 2) which may result in localizing groundwater flow. With regard to the Mesozoic sedimentary sequence, field observation and previous drilling experience in the area reveal that the Hamanlie Formation is highly fractured and, thus, it is the best hydrostratigraphic unit than other sedimentary rocks of the area. Approximately, east of 40.5° longitude the Hamanlie Formation is overlain by the relatively younger impermeable formations—the Urandab, Gebredarre, and Gorrahe Formations—leaving this potential aquifer beyond the reachable depth for economic drilling. In the area covered with the sedimentary rocks other than the Hamanlie Formation, groundwater occurs and moves in the alluvial sediments along dry riverbeds and flood plain of Dawa. In line with

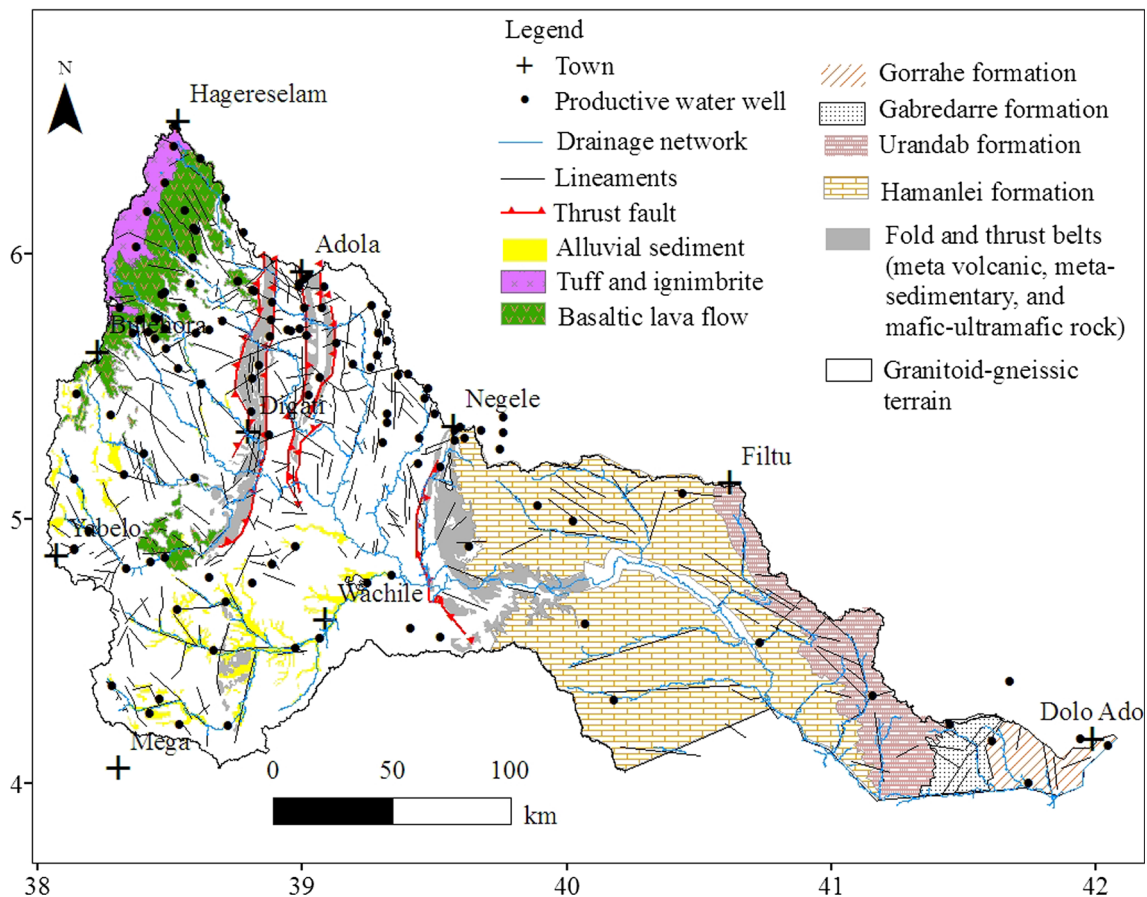


Fig. 2 Simplified geological map (lithology and fracture network) with plot of water scheme

surface inclination and dominant fracture orientations, the general groundwater flow direction is toward the southeast (Fig. 3b).

Methodology

Detailed analysis of the hydrochemical data together with the assessment of isotopic characteristics of groundwater was the principal methods used in this study. Existing geological and hydrogeological information were also used. Seventy-nine water samples were collected in the polyethylene bottles for the chemical analysis. Groundwater samples were collected from wells after 10 min of pumping. At each sampling point, the bottles were completely rinsed, at least two times, with the source waters to be sampled. Electrical conductivity (EC), total dissolved solids (TDS), pH, and groundwater temperature were measured on the spot using field measuring kits. Data acquired in this study were complemented by hydrochemical data from MoWIE (2007), Zewdie and Nahuseyay (2011), and Zewdie and Sima (2011). A total of 26 samples were collected in standard sampling bottles for the

determination of tritium. Twenty-one of these samples were collected from water wells and springs and 5 samples were from the local rainfall. Seventy-two groundwater samples were collected for the analysis of $\delta^2\text{H}$ and $\delta^{18}\text{O}$. In this case, the bottles were completely filled and then tightly capped and plastered around the mouth to avoid isotopic exchange with the atmosphere. By means of one-time sampling of the rainfall events, 15 samples of the local rainfall of March–April 2014 were collected for the analysis $\delta^2\text{H}$ and $\delta^{18}\text{O}$. Additional data of $\delta^2\text{H}$, $\delta^{18}\text{O}$, and tritium of the local rainfall and rainfall at Addis Ababa, Ethiopia, were obtained from International Atomic Energy Agency (IAEA) Global Network for Isotopes in Precipitation (GNIP) data base (<http://www.iaea.org/water>). Except alkalinity, all other major cations and anions, and environmental isotopes of the present sampling were analyzed in the laboratory of the School Earth Sciences (SES), Addis Ababa University. Calcium and magnesium were determined using a Jenway 6405 UV/Vis spectrophotometer, and sodium and potassium were determined by atomic absorption spectrophotometer. Sulfate ion was determined by a Jenway 6405 UV/Vis spectrophotometer for some of the samples and by ion chromatography for the

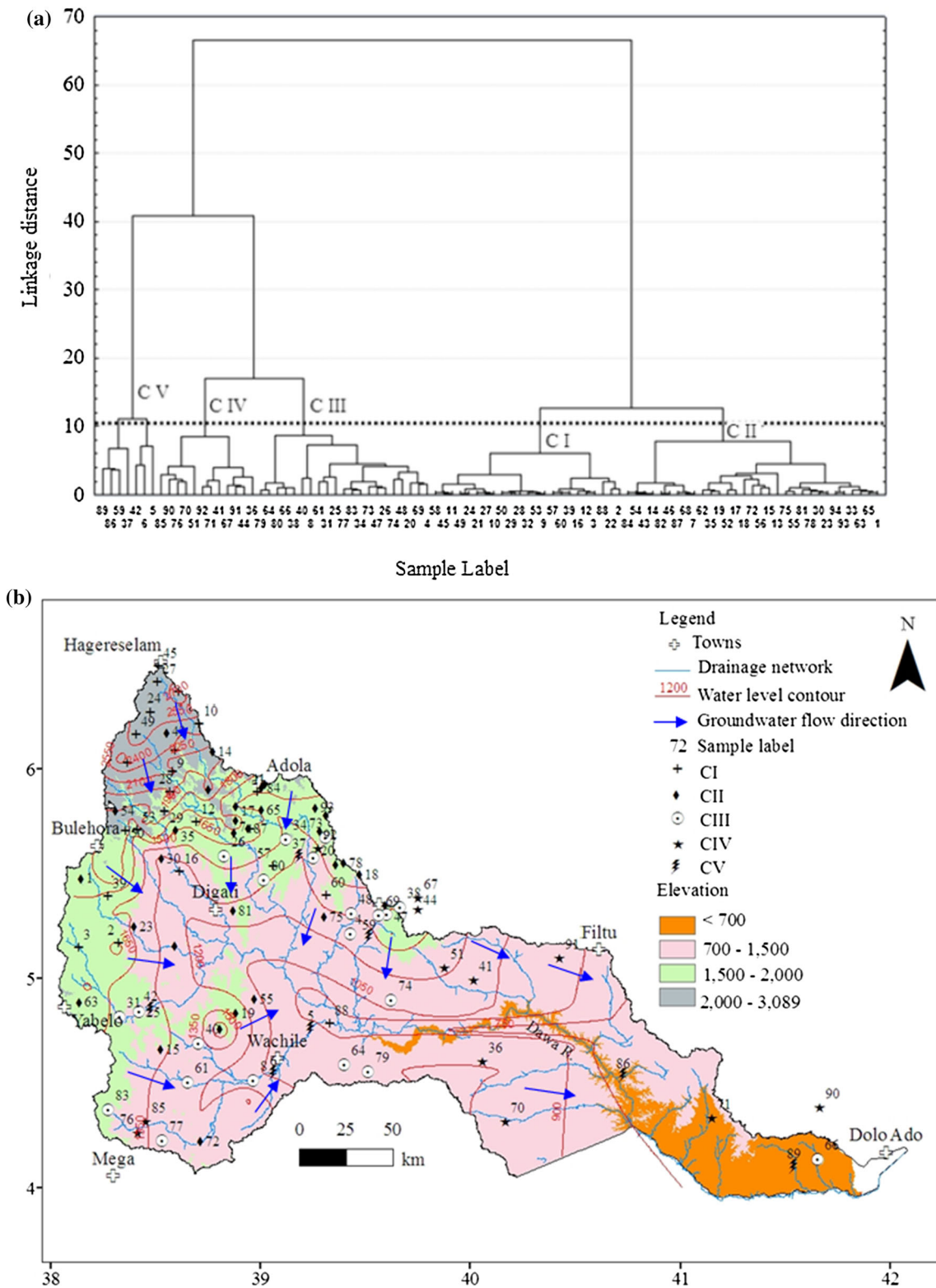


Fig. 3 **a** Dendrogram of HCA showing associations between samples (*line of asterisks is chosen by analyst to select number of sub-clusters*) **b** Spatial distribution of clusters (or samples) plotted along with elevation and groundwater flow direction

other samples. Chloride was determined partly by titration and partly by ion chromatography. Alkalinity was determined by titration immediately after sampling. For each analysis, analytical precision, expressed in standard deviation, is generally $\pm 4\%$. Accuracy of chemical analysis for the total measurements of ions was verified again by calculating the ionic balance errors and was generally within $\pm 10\%$. In this study, 94 chemical data with reaction error of $\pm 5\%$ were used. Stable isotopes ($\delta^{18}\text{O}$ and $\delta^2\text{H}$) and tritium (T) were determined, respectively, by Los Gatos DLT 100 Liquid–Water Isotope Analyzer (LWIA) and electrolytic enrichment and liquid scintillation spectrometry (EELSS). Standard deviation was $\pm 2\%$ for $\delta^2\text{H}$, $\pm 0.2\%$ for $\delta^{18}\text{O}$, and $\pm 0.5\sigma$ for tritium.

Hydrochemical data were analyzed statistically and graphically. The statistical technique used in this study is HCA. It is a technique to group a number of samples into clusters of distinct water quality controlled by typical hydrological and hydrogeological processes. A detailed description of the technique can be obtained in StatSoft Inc (2007). The effectiveness of the technique to classify water quality data into distinct clusters was proved in a number of studies (e.g. Kebede et al. 2005; Belkhiri et al. 2010; Demlie et al. 2007). In the present study, Statistica software version 8.0 (StatSoft Inc 2007) was used to cluster the samples considering 9 water quality variables (EC, pH, Na^+ , K^+ , Mg^{2+} , Ca^{2+} , Cl^- , HCO_3^- , and SO_4^{2-}). To know hydrochemical facies of the water samples, hydrochemical data were plotted on a Piper diagram (Piper 1944) using AquaChem software for Windows version 4.0.284 (Waterloo Hydrogeologic Inc 2003). The use of concept of hydrochemical facies to understand groundwater flow system is well illustrated in Glynn and Plummer (2005), and the concept was widely applied in number of previous studies (e.g. Kebede et al. 2005; Demlie et al. 2007; Zouari et al. 2011). Interpretation of isotope data was aided by plotting the data on the traditional $\delta^{18}\text{O}$ versus $\delta^2\text{H}$ graph along with the local and global meteoric water lines. For the illustration of spatial distribution of geological information and hydrochemical and isotope data, ArcGIS 10 graphic software was used.

Results and discussion

HCA was employed on the hydrochemical data set of 94 samples. Consequently, the water samples were classified into five statistically distinct clusters (C): CI, CII, CIII, CIV, and CV. The resultant dendrogram of HCA and the spatial distribution of the clusters are shown in Fig. 3a, b, respectively. Each of these clusters corresponds to a typical geologic and geographic environment. Preliminary description of the clusters is given as

follows based on the statistical summary of water quality parameters (Table 1).

CI is comprised of 23 samples largely collected from the highland volcanic terrain. Few samples of this cluster are associated with the relatively elevated region in the northwestern parts of the basement terrain (Fig. 3b). CI is represented by a mean EC of $331.2\ \mu\text{S}/\text{cm}$ (or TDS of $242\ \text{mg}/\text{l}$). CII is comprised of 31 samples many of which are collected from the northern half of the basement terrain. Some of the samples of this cluster are also related to the headwater region of the dry stream channel and near the foot of elevated areas in the southern half of the basement terrain (Fig. 3b). CII is characterized by mean EC equals $672.2\ \mu\text{S}/\text{cm}$ (or TDS equals $438\ \text{mg}/\text{l}$) showing slightly higher salinity than CI. In both CI and CII, Ca^{2+} and HCO_3^- are the dominant ions with the other cations and anions existing in appreciable amount. CIII is comprised of 21 samples where many of the samples are sited at some distance downstream of the hill-foot or away from head water of the dry riverbed in the semiarid southern half of the basement terrain. The mean EC and TDS of CIII is $1523.2\ \mu\text{S}/\text{cm}$ and $1000\ \text{mg}/\text{l}$, respectively. As in CI and CII, HCO_3^- is the most abundant anion in CIII samples; however, in CIII, Na^+ is the most abundant cation with important amount of Ca^{2+} and Mg^{2+} (Table 1).

CIV consists of 12 samples that have been largely collected from the sedimentary terrain (Fig. 3b). Two samples of this cluster are associated with dry stream beds in the southern half of the basement terrain. In CIV, the mean EC or TDS is high ($2606.3\ \mu\text{S}/\text{cm}$ or TDS, $1728.0\ \text{mg}/\text{l}$), respectively, and SO_4^{2-} is the most abundant anion followed by HCO_3^- and Cl^- . CV is comprised of 7 samples in which all are associated with the dry riverbeds in the semiarid and arid part of the study area (Fig. 3b). This cluster is characterized by very high mean EC ($7526\ \mu\text{S}/\text{cm}$) or TDS ($4739.1\ \text{mg}/\text{l}$), and Na^+ is the most abundant cation followed by Ca^{2+} , Mg^{2+} , and K^+ . The most abundant anion is SO_4^{2-} followed by Cl^- and HCO_3^- (Table 1). In the study area, EC of the samples or of the clusters is related to the respective TDS by factors which are in the range 0.60–0.66. This range of factors is within the range of factors, 0.50–0.75, established for natural waters by Walton (1989). This signifies that TDS and EC can be used interchangeably in the subsequent discussion.

TDS and the relative percentage of cations and anions can be used to infer the scale of groundwater flow systems. Based on theory (Toth 1984) and field observations (Ophori and Toth 1989) low TDS and high percentage of Ca, Mg, and HCO_3^- are associated with local flow systems; intermediate TDS and high percentage of Na^+ , SO_4^{2-} , and Cl^- are characteristics of intermediate flow systems; and high TDS and high percentages of Na^+ and Cl^- are characteristics of regional flow systems. In the view of that,

Table 1 Statistical summary of hydrochemical parameters of groundwater of clusters resulted from Q-mode HCA analysis (*EC in $\mu\text{S/cm}$; cations and anions in mg/l ; temperature in $^{\circ}\text{C}$; and % is percent of ions relative to corresponding cations and anions*)

C	Variables	PH	Temp	TDS	EC	Ca	Mg	Na	K	HCO ₃	Cl	SO ₄	No. of samples (n)
I	Minimum	6.6	17.1	60.0	97.0	10.6	2.0	5.0	1.4	55.6	1.8	0.0	23
	Maximum	7.5	24.9	682.0	887	131.9	25.0	58.0	9.0	317.2	32.3	296.0	
	Mean	7.0	20.8	214.6	331.2	43.2	9.0	16.1	3.7	169.1	10.7	28.6	
	SD	0.2	2.1	149.0	212.0	29.4	6.3	12.0	2.1	79.8	9.3	64.3	
	%					60.0	12.5	28.9	5.1	81.1	5.1	13.7	
II	Minimum	5.5	18.3	26.0	42.0	4.2	1.0	1.9	0.3	21.5	1.0	0.0	31
	Maximum	6.9	28.0	1019.0	1559.0	166.0	62.0	212.0	26.0	482.1	186.2	217.9	
	Mean	6.5	23.1	437.9	676.2	63.7	18.2	48.8	4.8	231.6	56.2	64.3	
	SD	0.3	2.2	252.2	393.0	41.6	13.3	42.6	5.9	117.4	59.2	69.7	
	%					47.0	13.4	36.0	3.5	65.8	16.0	18.3	
III	Minimum	6.3	21.7	418.0	640.0	9.0	8.4	6.0	0.5	294.0	6.0	2.0	21
	Maximum	8.0	28.5	1766.0	2943.0	285.0	124.0	420.0	39.0	1002.0	443.0	625.0	
	Mean	7.2	25.5	999.7	1523.2	115.2	49.5	134.6	13.3	577.9	128.1	115.4	
	SD	0.5	1.7	430.8	678.6	70.4	27.3	105.8	12.6	164.9	121.9	153.6	
	%					36.9	15.8	43.1	4.3	70.4	15.6	14.1	
IV	Minimum	6.4	23.0		1536.0	75.0	80.0	29.0	1.0	225.0	16.0	484.0	12
	Maximum	7.7	29.0		4853.0	398.0	222.0	523.0	44.0	652.0	701.0	2039.0	
	Mean	7.1	26.6		2606.3	252.6	143.1	210.3	15.3	381.1	265.7	941.7	
	SD	0.4	1.6		1079.5	114.0	39.8	181.6	13.5	111.7	256.4	437.8	
	%					40.7	23.0	33.8	2.5	24.0	16.7	59.3	
V	Minimum	6.7	24.9		4647.0	82.0	82.7	640.0	5.0	231.0	752.3	714.5	7
	Maximum	7.8	28.4		9970.0	1002.0	289.0	1562.0	110.0	1110.0	1901.0	2540.0	
	Mean	7.1	26.8		7526.4	408.1	201.9	976.7	36.7	545.6	1345.7	1552.0	
	SD	0.4	1.2		2036.1	308.3	77.5	290.5	39.7	279.6	372.5	751.5	
	%					25.1	12.4	60.2	2.3	15.8	39.1	45.1	

chemical character of CI and CII suggests the local groundwater flow systems in the highland regions of volcanic and basement terrain of the study area. The chemical characteristics of CIII are also comparable to that of the local groundwater flow system though Na⁺ concentration is slightly higher than Ca²⁺ or Mg²⁺ (Table 1). However, the high percentage of Na⁺ is not beyond expectation given the dominance of rocks of felsic composition in the southern half of the basement terrain.

Additionally, hydrochemical data are plotted on a Piper diagram (Piper 1944) (Fig. 4) to make detailed analysis of water quality in terms of hydrochemical facies. Subsequently, the classification scheme of Back (1966) was used to group the water samples into different chemical types of water based on the dominant ions. The approach is widely used in many previous hydrogeological studies (e.g. Ophori and Toth 1989; Adams et al. 2001; Güler et al. 2002; Kebede et al. 2005). Accordingly, a wide variety of water types was found in the volcanic and basement terrains of the study area that is represented by CI, CII, and CIII

(Table 2). However, mixed cation–bicarbonate, (Ca, Mg, Na)–HCO₃, water type dominantly occurs in these areas with the type of dominant cation varying from sample to sample based on the local geology. Moreover, in these clusters, the majority of the samples have a cation composition characterized by a Ca²⁺+Mg²⁺ higher than Na⁺+K⁺ (Fig. 4a–c). In particular, 91 % of CI samples are HCO₃ type. Of these HCO₃-type samples, 74 % is Ca–HCO₃ type followed by 17 % of mixed cation–HCO₃-type water. Likewise, 67 % of the samples of CII and CIII are HCO₃ type (Table 2). Based on groundwater chemical evolution models (Adams et al. 2001; Kebede et al. 2007), chemical character of CI, CII, and CIII indicates that in the most parts of the volcanic and basement terrain of the study area, groundwater is at the early stages of geochemical evolution (recent recharge) or rapidly circulating which has not undergone significant water–rock interactions.

On the other hand, 67 % of the samples of CIV are sulfate type where 25, 17, and 25 % of these samples are Ca–SO₄, Mg–SO₄, and mixed–SO₄ type, respectively

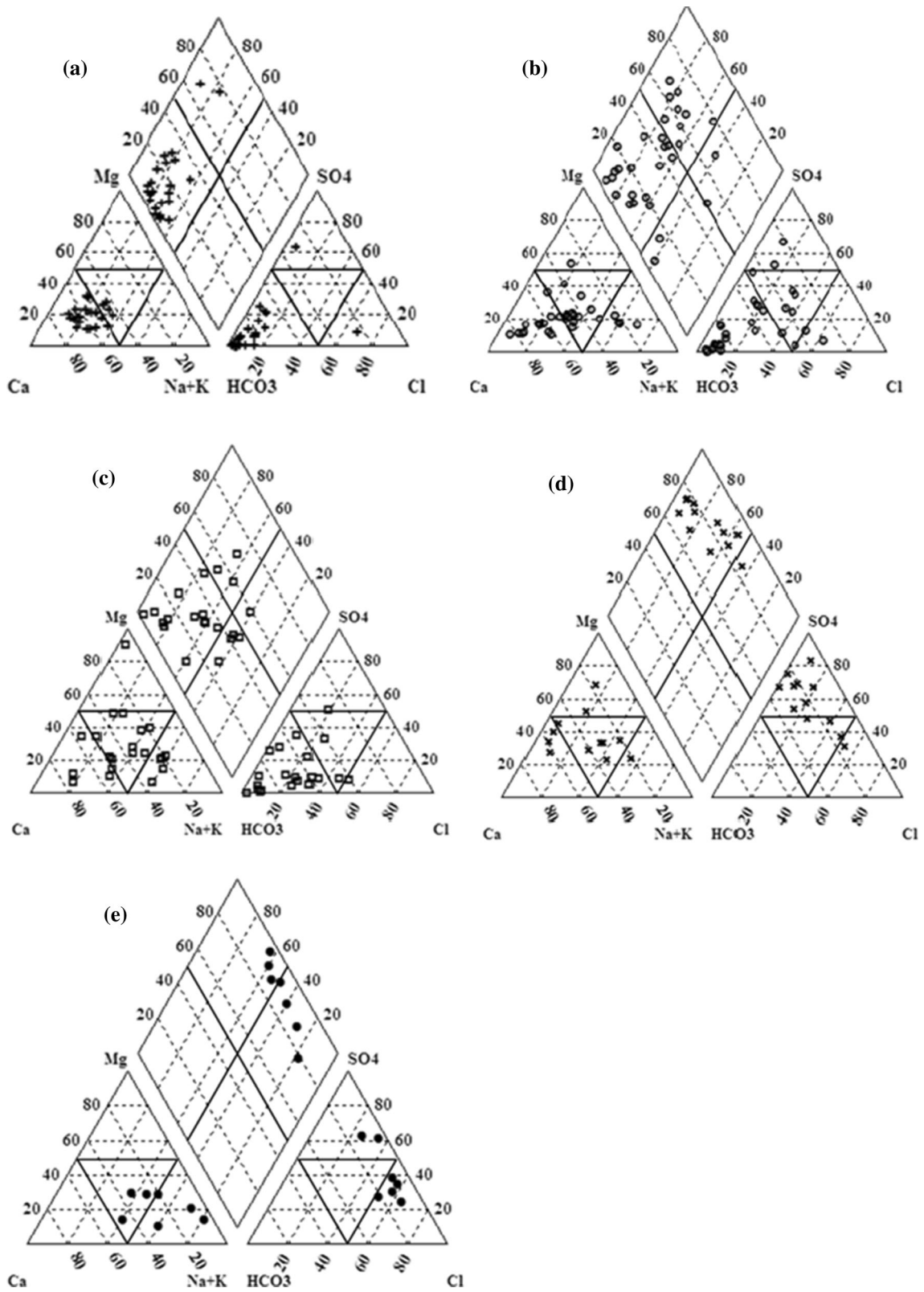


Fig. 4 Piper plot of hydrochemical data: **a** CI; **b** CII; **c** CIII; **d** CIV; and **e** CV

Table 2 Groundwater types

Cluster	Cation type	Anion type	Water type
CI (<i>n</i> = 23)	Ca type (83 %, <i>n</i> = 19) Mixed type (17 %, <i>n</i> = 4)	HCO₃ type (91 %, <i>n</i> = 21) SO ₄ type (4 %, <i>n</i> = 1) Cl type (4 %, <i>n</i> = 1)	Ca–HCO ₃ (74 %, <i>n</i> = 17) Mixed cation–HCO ₃ (17 % <i>n</i> = 4) Ca–SO ₄ (4 %, <i>n</i> = 1) Ca–Cl (4 %, <i>n</i> = 1)
CII (<i>n</i> = 31)	Ca type (39 %, <i>n</i> = 12) Mixed type (45 %, <i>n</i> = 14) Mg type (3 %, <i>n</i> = 1) Na type (13 %, <i>n</i> = 4)	HCO₃ type (61 %, <i>n</i> = 19) Mixed type (29 %, <i>n</i> = 9) SO ₄ type (7 %, <i>n</i> = 2) Cl type (3 %, <i>n</i> = 1)	Ca–HCO ₃ (23 %, <i>n</i> = 7) Mixed cation–HCO ₃ (29 %, <i>n</i> = 9) Mg–HCO ₃ (3 %, <i>n</i> = 1) Na–HCO ₃ (3 %, <i>n</i> = 1) Mixed cation–SO ₄ (7 %, <i>n</i> = 2) Na–Cl (3 %, <i>n</i> = 1) Ca–mixed anion (16 %, <i>n</i> = 5) Na–mixed anion (3 %, <i>n</i> = 1) Mixed cation–mixed anion (3 %, <i>n</i> = 1)
CIII (<i>n</i> = 21)	Ca type (19 %, <i>n</i> = 4) Mixed type (52 %, <i>n</i> = 11) Na type (24 %, <i>n</i> = 5) Mg type (5 %, <i>n</i> = 1)	HCO₃ type (76 %, <i>n</i> = 16) Mixed type (14 %, <i>n</i> = 3) SO ₄ type (5 %, <i>n</i> = 1) Cl type (5 %, <i>n</i> = 1)	Ca–HCO ₃ (19 %, <i>n</i> = 4) Na–HCO ₃ (14 %, <i>n</i> = 3) Mixed cation–HCO ₃ (38 %, <i>n</i> = 8) Mg–HCO ₃ (5 %, <i>n</i> = 1) Na–mixed anion (10 %, <i>n</i> = 2) Mixed cation–mixed anion (5 %, <i>n</i> = 1) Mixed cation–Cl (5 %, <i>n</i> = 1) Mixed cation–SO ₄ (5 %, <i>n</i> = 1)
CIV (<i>n</i> = 12)	Ca type (25 %, <i>n</i> = 3) Mg type (17 %, <i>n</i> = 2) Na type (8 %, <i>n</i> = 1) Mixed type (50 %, <i>n</i> = 6)	SO₄ type (67 %, <i>n</i> = 8) Mixed type (25 %, <i>n</i> = 3) Cl type (8 %, <i>n</i> = 1)	Ca–SO ₄ (25 %, <i>n</i> = 3); Mg–SO ₄ (17 %, <i>n</i> = 2); Mixed cation–SO ₄ (25 %, <i>n</i> = 3) Na–Cl (8 %, <i>n</i> = 1); Mixed cation–mixed anion (25 %, <i>n</i> = 3)
CV (<i>n</i> = 7)	Na type (43 %, <i>n</i> = 3) Mixed type (57 %, <i>n</i> = 4)	Cl type (71 %, <i>n</i> = 5) SO ₄ type (29 %, <i>n</i> = 2)	Na–Cl (42 %, <i>n</i> = 3) Mixed cation–Cl (29 %, <i>n</i> = 2) Mixed cation–SO ₄ (29 %, <i>n</i> = 2)

(Table 2). In particular, all waters collected from the wells that penetrate into the Hamanlie sedimentary formation show chemical character of sulfate type. Since Ca²⁺ + Mg²⁺ is greater than Na⁺ + K⁺ (Fig. 4d), the chemical character of these waters is better explained in terms of dissolution of gypsum by locally recharged water rather than geochemical evolution associated with the groundwater flow. Sulfate-type water is also observed at a few locations in the fold and thrust belts of the basement terrain (e.g., sample labeled 13 and 84). In this case, source of sulfate is plausibly associated with oxidation of sulfide minerals. This is supported by the observation of low-pH waters in the area. pH as low as 4.5 is observed at sample labeled 13. Furthermore, in geological literatures (e.g. Hamrla 1977) occurrence and oxidation of sulfide minerals is reported in this part of the study area.

Further, no clear signature of geochemical evolution is observed from CI through CII to CIII along N–S hypothetical transect or from CI through CII to CIV along NW–SE

hypothetical transects. This presumably supports the absence of continuous flow system from the northern highland volcanic and basement terrain toward southern basement and southeastern sedimentary terrain. If there were regional or continuous groundwater flow systems between these two regions, there would be geochemical evolution sequentially changing along the flow lines in the order of HCO₃[−] → HCO₃[−] + SO₄^{2−} → SO₄^{2−} + HCO₃[−] → SO₄^{2−} + Cl[−] → Cl[−] + SO₄^{2−} → Cl[−] as suggested by Chebotarev (1955).

In addition, the occurrence of groundwater with variable composition within the short distance between the sampling points, as illustrated by the spatial plot of EC, HCO₃[−], and SO₄^{2−} + Cl[−] (Fig. 5a–c), supports the localized/discrete groundwater flow system in the basement terrain.

In most of the selected samples of CI, CII, CIII, and CIV, tritium varies between 1.45 and 3.18TU. This range of tritium value is equivalent to the range of tritium amount in the local rainfall which varies between 1.27 and 4.1TU

Fig. 5 Spatial variation of EC (a), HCO_3^- (b), and $\text{SO}_4^{2-} + \text{Cl}^-$ (c) in mg/l

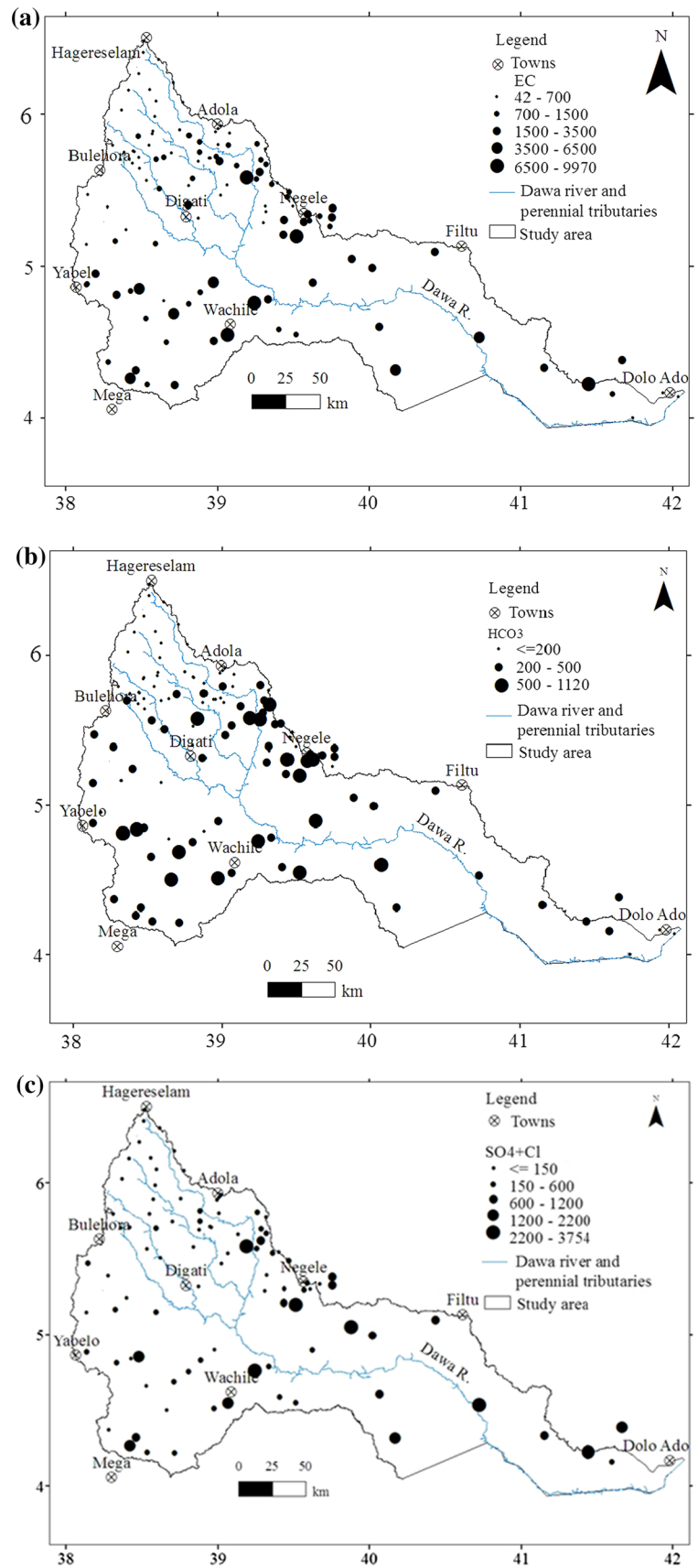
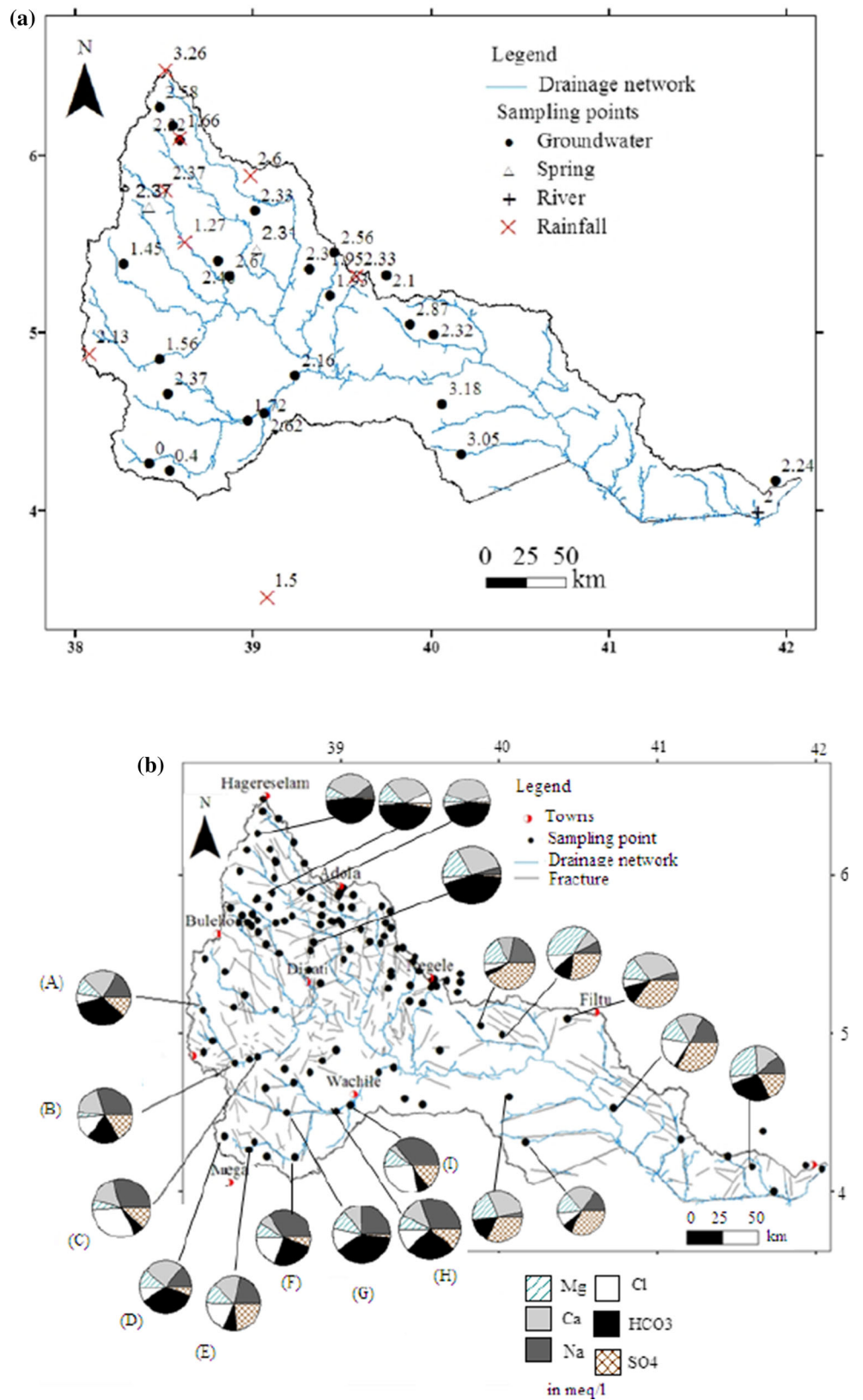


Fig. 6 **a** Sampling locations for tritium (*number* indicates tritium value); **b** chemical characteristics along selected dry riverbeds: A–C, G–I, and D–E



(Fig. 6a). The observation of appreciable amount of tritium in the groundwater of the basin at levels comparable to the local rainfall also indicates that groundwater is of local origin, with modern recharge, and a short aquifer residence time in the most parts of the study area.

Exceptionally, based on Ophori and Toth (1989), CV samples and the two samples of CIV (sample labeled 76 and 77) which are sited at few locations along the dry riverbeds are marked with chemical character of intermediate flow systems. On the other hand, based on groundwater chemical evolution models (Kebede et al. 2005; Demlie et al. 2007), chemical character of this water suggests groundwater at its later stage of geochemical evolution which might be associated with the extended flow distance along the dry riverbeds. For example, site *C* and *I* (Fig. 6b) are represented by two of CV samples and site *E* (Fig. 6b) is represented by one of CIV samples. A progressive change in chemical composition from calcium bicarbonate type to sodium chloride or to sulfate-type water is observed along *A–B–C*, *D–E*, and *G–H–I* dry stream beds (Fig. 6b), signifying chemical evolution. However, the tritium amount at site *C*, 1.56TU, and *I*, 1.76TU, is at amount comparable to the local rainfall, indicating modern groundwater recharge and fast groundwater circulation. This suggests that it is unlikely that chemical evolution, associated with long flow distance, has caused the changes in the water chemistry along the dry riverbeds *A–B–C* and *G–H–I*. As discussed below, the isotopic data of groundwater at site *C* and *I* and of other samples which are sited along the dry riverbeds and marked with higher EC are plotted in the right side below the LMWL, signifying the importance of evaporation in modifying water chemistry. On the other hand, Cl^-/Br^- ratio, in mg/l, of the high EC water in the semiarid region in general, which includes CV samples, is less than 400. It is only the sample at site *I*, which is marked with the relatively high ratio, i.e., 1000. Low values of Cl^-/Br^- ratio in the groundwater is frequently explained by the absence of halite dissolution because water affected by salt dissolution will have ratio greater than 1900, and the ratio will be as high as 100,000 if pure halite is involved (Davis et al. 1998). Furthermore, according to MoWIE (2007), the EC of the soil tested at three sites along *G–H–I*, including site *I*, is less than 0.4 mS/cm, indicating salt content in the soil is low. These observations likely lead to the conclusion that evaporative enrichment has significant effect over halite dissolution to control water chemistry in CV samples.

However, the tritium amount is exceptionally low at site *E* (Fig. 6b), indicating that relatively old water is present at this site. Subsequently, variations in the composition of groundwater along the line *D–E* (Fig. 6b) can be explained by chemical evolution associated with long groundwater residence time. The long groundwater residence time and,

hence, the low tritium value at site *E*, are likely to be associated with the high clay content and the low hydraulic conductivity of the formation of this particular area. Belete et al. (2000) reported that in this part of the study area Quaternary sediments which is as thick as 50 m and composed of dominantly clay associated with marl and mudstone fill the valley bottom. According to the MoWIE (2007), the sediments in the area constitutes up to 59 % clay. Generally high clay proportion lowers hydraulic conductivity (Heath 1983). Besides, low well yield, 0.7 l/s at site *E* and 0.5 l/s at site *D*, even lower, 0.1 l/s, in the surrounding area (Belete et al. 2000) supports the low hydraulic conductivity in the area. However, further downstream at site *F*, continuity of geochemical evolution was not observed (Fig. 6b) due to structural discontinuity that results local variations in the groundwater flow system.

Generally, the aforementioned hydrochemical results and subsequent discussions accompanied with tritium data illustrate the dominance of local flow system in the much areas of volcanic, basement, and sedimentary terrain of the study area. In general, these data support the view that groundwater in the region occurs in local flow system that receive localized recharge.

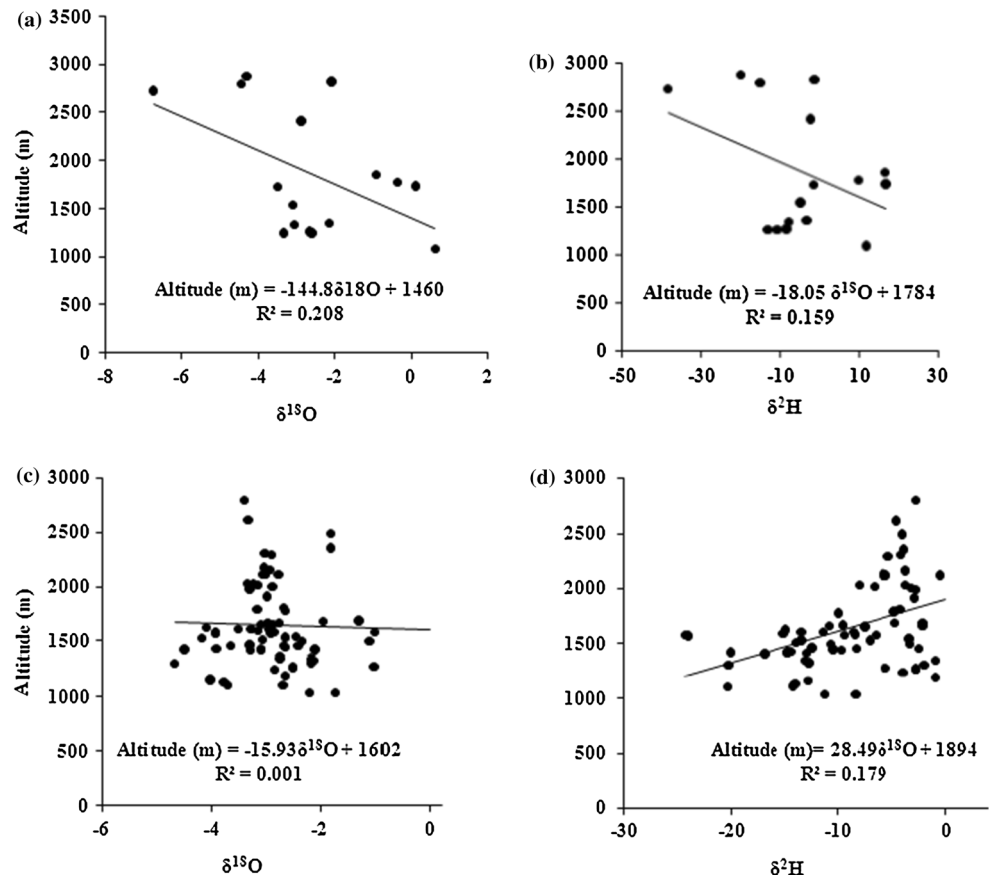
Earlier, it is revealed that there is a general increase in mean EC or TDS from CI to CV. Increases in the mean EC or TDS are likely to be related to the difference in the local hydrogeological, physiographic, and climatic factors. The northern highland volcanic and basement region is dominantly characterized by fractured aquifer systems, rugged topography, and humid to sub-humid climatic conditions. On the other hand, southern part of the basement terrain is characterized by relatively flat topography, semiarid climatic conditions, and water movement through the alluvial sediments. By implication, there is high contact area and contact time between rock and water, and substantial amount of dissolvable salts in the aquifer matrix of southern basement terrain than the northern highland region. As a result, groundwater samples from southern part of the basement terrain (CIII and CV) are characterized by the relatively high mean EC or TDS than that of groundwater in the northern highland (CI and CII). In CIV, the high EC likely associated with evaporite, such as gypsum, dissolution. In various studies elsewhere (e.g., Back 1966; Demlie et al. 2007), the general increase in TDS or EC was explained by regional groundwater flow system. However, this study illustrates increase in EC or TDS alone might not always display regional flow system.

Stable isotope ($\delta^2\text{H}$ and $\delta^{18}\text{O}$) data have been analyzed to supplement the results of hydrochemical and tritium data analysis. Using the records of stable isotopes of rainfall of the study area (number of data points = 48), regression analysis between $\delta^2\text{H}$ and $\delta^{18}\text{O}$ forms the local meteoric water line (LMWL) for the southern Ethiopia

Table 3 Summary of environmental isotopes of groundwater of the study area

	Minimum ($\delta^2\text{H}$, $\delta^{18}\text{O}$)	Maximum ($\delta^2\text{H}$, $\delta^{18}\text{O}$)	Median ($\delta^2\text{H}$, $\delta^{18}\text{O}$)	Mean ($\delta^2\text{H}$, $\delta^{18}\text{O}$)	Stdev ($\delta^2\text{H}$, $\delta^{18}\text{O}$)	N
Entire area	(-24.21, -4.69)	(-0.55, -1.01)	(-9.99, -2.99)	(-9.93, -2.93)	(5.84, 0.74)	62
Northern highland	(-15.09, -3.5)	(-0.55, -1.10)	(-4.5, -2.88)	(-5.26, -2.70)	(3.17, 0.57)	31
South-central and southeastern region	(-24.21, -4.69)	(-9.45, -1.01)	(-13.88, -3.22)	(-14.64, -3.22)	(3.92, 0.82)	31

Fig. 7 Altitude versus stable isotope of rainfall of the study area: **a, b** altitudinal variations of stable isotopes in groundwater of the study area **c, d**



that is expressed by equation: $\delta^2\text{H} = 6.645\delta^{18}\text{O} + 11.69$ ($R^2 = 0.853$). A statistical summary of isotopic composition of rainfall of the study area and of the selected region in the basin is given in Table 3. Rainfall in the southern and southeastern lowland is more isotopically enriched than that of the northern highland parts of the study area (Table 3). Depletion in isotopic composition of the local rainfall with rise in altitude is also observed (Fig. 7a, b) based on the isotopic data obtained by means of one-time sampling of local rainfall events. In general, altitudinal depletion in the isotopic composition of rainfall of the study area complies with altitude–isotope relationship of Ethiopian rainfall (Kebede 2013).

In the groundwater of the study area, $\delta^2\text{H}$ varies between -24.21 and -0.55 ‰ and $\delta^{18}\text{O}$ varies between -4.69 and

-1.01 ‰ (Table 3). Unlike observations from other regions in Ethiopia where $\delta^{18}\text{O}$ in the groundwater is depleted along with increase in altitude with average depletion rate of -0.1 ‰/100 m (Kebede et al. 2005, 2007), $\delta^{18}\text{O}$ in the groundwater of the study area is not well correlated with altitude (Fig. 7c) and a plot of $\delta^2\text{H}$ versus altitude shows groundwater is slightly enriched in $\delta^2\text{H}$ along with rise in altitude (Fig. 7d). Furthermore, both the range, median, or mean values of the stable isotopes (Table 3) and plot of the data on $\delta^2\text{H}$ versus $\delta^{18}\text{O}$ diagram along with meteoric water lines (Fig. 8) show that groundwater in the south-central and southeastern parts of the study area are isotopically depleted relative to groundwater in the northern highland. Analogs to the isotopic depletion of the local rainfall with rise in altitude,

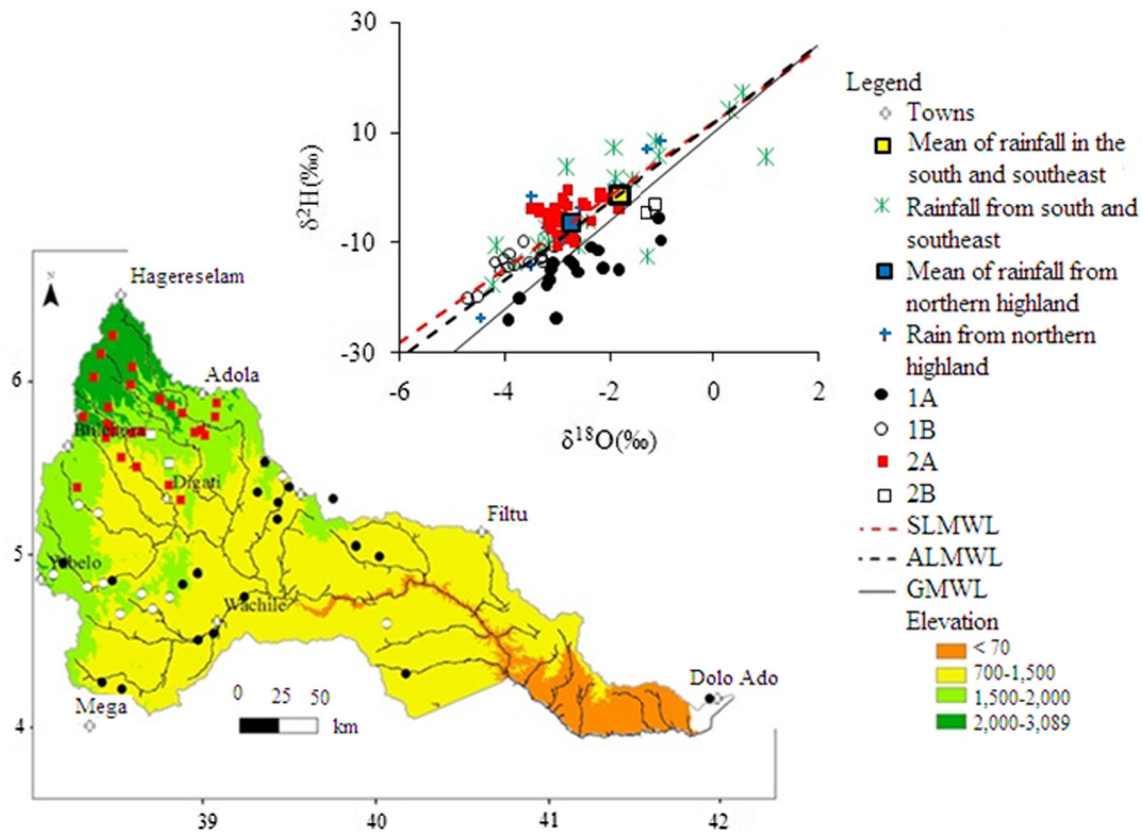


Fig. 8 Plot of isotope data on $\delta^2\text{H}$ versus $\delta^{18}\text{O}$ diagram along with spatial distribution (1A = evaporated southern and southeastern groundwater; 1B = non-evaporated southern and southeastern

groundwater; 2A = highland non-evaporated groundwater; 2B = evaporated highland groundwater; SLMWL = LMWL of southern Ethiopia; and ALMWL = LMWL at Addis Ababa)

groundwater of the northern highland region would have been isotopically depleted relative to groundwater in the southern and southeastern parts of the study area.

According to Gat (2010), as long as temperature of groundwater system is less than 60 °C, the isotopic composition of groundwater is not modified due to interaction with aquifer material. In general, groundwater of the study area is characterized by low temperature, 17.1–29 °C. Given this local physical condition and the general groundwater flow direction toward southeast, isotopic depletion in groundwater of the southern, south-central, and southeastern parts of the study area relative to the groundwater in the northern highland signifies distinct recharge source and absence of flow continuity between the two regions. This supports what deduced from the analysis of hydrochemical and tritium data.

Despite the converging evidences from hydrochemical, stable isotope, and tritium data support recharge of local origin, groundwater in the semiarid southern and southeastern parts of the study area is plotted in the depleted side of $\delta^2\text{H}$ versus $\delta^{18}\text{O}$ diagram relative to the local rainfall (Fig. 8). This implies that recharge only takes place from

isotopically depleted high-intensity local rainfall events. The high-intensity rainfall must activate flush floods that subsequently result in the groundwater recharge in the valley bottoms and along dry riverbeds. This finding is in line with the regional work of Kebede (2013) that provided the regional picture of mechanism of groundwater recharge in Ethiopia. Elsewhere, recharge from flush floods has been also observed to cause an isotopic depletion of groundwater as compared to precipitation under arid conditions (Leibundgut et al. 2009; Gat 2010). This typical recharge mechanism in the semiarid parts of the study area is the likely causes of the disparity in altitude–isotope relationship of the study area from the observations elsewhere in Ethiopia.

On the standard $\delta^2\text{H}$ versus $\delta^{18}\text{O}$ graph, groundwater samples, which are collected from the northern highland area and includes selected samples of CI and CII in the area, are plotted around the mean isotopic composition of the local rainfall within the constricted range on or near the LMWL (2A samples, Fig. 8). This suggests infiltration of the local rain water is significantly rapid before evaporation takes place and a fairly invariable isotopic composition,

and the most likely well-mixed system. Exceptionally, two groundwater samples of the highland region are plotted on the right side below the LMWL (2B samples, Fig. 8). Field observation reveals that these samples were collected from the water wells located in the vicinity of marshy ground. The shallow groundwater in the marshy area, which plausibly subjected to direct evaporation has likely influenced the isotopic composition of the groundwater at the sampling site.

As in highland area in the north, many of the samples, which were collected from an elevated area and near foothills in the semiarid region in the southwest and south-central areas of the river basin and include selected samples of the area that belongs to CII, are also plotted on or near the LMWL (1B samples, Fig. 8) pinpointing the insignificance of evaporation losses before, during, or after recharge. However, a large number of groundwater samples, which were collected from the semiarid region and include selected samples in CIII, CIV, and CV, are plotted on the right side below the LMWL (1A samples, Fig. 8). This indicates the importance of evaporation losses before, during, or after recharge process along dry riverbeds and at few locations in the sedimentary terrain. Variation in the intensity of evaporation between 1A and 1B groundwater can be explained in terms of variation in evaporation regime. In the elevated area and near the hill-foot, temperature is relatively low and the floodwater stays on the ground surface for the short period of time before recharge takes place. As a result, the isotopic composition of the recharge water or of groundwater is not or less influenced by evaporation. However, further downstream toward south and southeast temperature increases along with fall in elevation and the floodwater exposes to evaporation regime for the longer time period. Consequently, this continuously enriches the isotopic composition in recharge water or groundwater of the area.

Conclusions

The Dawa River basin in southern Ethiopia is underlain by a crystalline basement complex, sedimentary formations, and volcanic rocks. The statistical analysis and graphical plots of hydrochemical and isotopic data have provided insights into the nature of groundwater recharge and flow system in the basin.

The low EC and TDS and the high percentage of $\text{Ca}^{2+} + \text{Mg}^{2+}$ over $\text{Na}^+ + \text{K}^+$ and HCO_3^- over $\text{SO}_4^{2-} + \text{Cl}^-$ in the groundwater of volcanic and most parts of basement terrain of the study area demonstrate the dominance of local groundwater flow systems. Moreover, large variations in groundwater chemical composition over short distances in fractured rock aquifers in the basement

terrain support the view that groundwater flow systems are localized in nature in the region. The dominance of Ca-HCO_3 and $(\text{Ca}, \text{Mg}, \text{Na}, \text{K})\text{-HCO}_3$ -type water in the volcanic and most parts of the basement terrain, respectively, signifies recent recharge or rapidly circulating groundwater in these parts of the study area. The presence of Ca^{2+} and Mg^{2+} at important amount in the high-sulfate groundwater of the sedimentary terrain reveals dissolution of gypsum by locally recharged rainfall than geochemical evolution. Supporting the results of hydrochemical analysis, the presence of tritium in the groundwater of all terrains at amount comparable to that in the modern local rainfall also signifies groundwater of local origin, modern recharge, and short residence time in the most parts of the study area. Exceptionally, there are sites with chemical character of extended flow system and signature of geochemical evolution along certain dry riverbeds in the semiarid parts of the study area. However, the presence of appreciable amount of tritium in the groundwater rules out likely the geochemical evolution along the flow lines. At one location in the south end, however, tritium amount is low, indicating groundwater of long residence time which is likely associated with groundwater flow in the lithologic unit of low hydraulic conductivity.

Overall, there is no signature of geochemical evolution that indicates the presence of continuous or regional flow system along N-S and NW-SE hypothetical transects. This deduction is also supported by the isotopic analysis in that, given the low-temperature groundwater system and the general groundwater flow direction toward southeast, isotopic depletion of groundwater in semiarid region in the south and southeast relative to groundwater in the humid highland in the north reasonably indicates the absence of flow continuity between the two regions.

Under semiarid climatic condition in the south and southeast, despite the source of recharge is the local rainfall, groundwater is depleted in $\delta^{18}\text{O}$ and $\delta^2\text{H}$ relative to the normal local rainfall, suggesting that recharge occurs only from isotopically depleted heavy rainfall. In the semiarid region at far distance downstream away from the hill-foot or elevated areas, evaporation prior to or after recharge is significant as evidenced from the plot of stable isotope data on the right side below the LMWL. Evaporation prior to or after recharge is insignificant in the humid region in the north as evidenced from the plot of stable isotopic data of the area on or near the LMWL.

Overall, converging evidences from different techniques indicate the dominance of local recharge and flow system in most parts of the study basin. The traditional regional groundwater flow model which is common in most large river basins of Ethiopia does not hold true in the Dawa River basin. The existence of a Precambrian basement

complex in the middle part of the basin likely makes the flow system discontinuous. More solid conclusion can be made from detailed tracer, litho-structural, geophysical, and hydrogeological investigation accounting temporal variation of groundwater dynamics. The result of this study has significant implication on groundwater development and management activities of the area.

Acknowledgments The authors are grateful to School of Earth Sciences, Addis Ababa University, for the support of field work and laboratory facility. The contribution of Guji and Borana Zone water resources office for the success of field work is also appreciative. Thanks to National Meteorological Agency for the provision of climatic data. Thanks to Dagimawi, Adane, and Dr. Nicolo for the assistance in analyzing hydrochemical and isotope samples. Special thanks also go to Uruga, Gumi, Satana, Adan, and Abdulshikur for the support during field activity.

References

- Abdelsalam MG, Stern RJ (1996) Sutures and shear zones in Arabian–Nubian shield. *J Afr Earth Sci* 23(3):289–310
- Adams S, Titus R, Pietersen K, Tredoux G, Harris C (2001) Hydrochemical characteristics of aquifers near Sutherland in the Western Karoo, South Africa. *J Hydrol* 241:81–93
- Assefa G (1988) Potential hydrocarbon-generating rock units within the Phanerozoic sequence of the Ogaden basin, Ethiopia: a preliminary assessment using the LOPATIN model. *J Pet Geol* 11(4):461–472
- Back W (1966) Hydrochemical facies and groundwater flow patterns in northern part of Atlantic Coastal Plain. United States Geological Survey professional paper 498-A
- Belete Y, Abaire B, Asfaw B, Tigabe M, Shiferaw D, Belachew A, Abdela M (2000) Hydrogeological, geophysical, and engineering geological investigation of Yabelo sheet (NB 37-14). Institute of Geological survey of Ethiopia, Addis Ababa
- Belkhir L, Boudoukha A, Mouni L, Baouz T (2010) Application of multivariate statistical methods and inverse geochemical modeling for characterization of groundwater—a case study: Ain Azel plain (Algeria). *Geoderma* 159:390–399
- Bisson RA, Lehr JH (2004) Modern groundwater exploration: discovering new water resources in consolidated rocks using innovative hydrogeologic concepts, exploration, drilling, aquifer testing, and management methods. Wiley, New Jersey
- Bugliosi EF (1999) The Midwestern Basins and Arches regional aquifer system in parts of Indiana, Ohio, Michigan, and Illinois. U.S. Geological Survey Professional Paper 1423-A
- Chebotaev II (1955) Metamorphism of natural waters in the crust of weathering. *Geochim* 8:22–28
- Dalton MG, Upchurch SB (1978) Interpretation of hydrochemical facies by factor analysis. *Groundwater* 16(4):228–233
- Danskin WR (1998) Evaluation of the hydrologic system and selected water-management alternatives in the Owens, Valley, California. U.S. Geological Survey Water supply Paper 2370-H
- Davis SD, Whittemore DO, Fabryka-Martin J (1998) Uses of chloride/bromide ratios in studies of potable water. *Groundwater* 36(2):338–350
- Demlie M, Wöhnlich S, Wisotzky F, Gizaw B (2007) Groundwater recharge, flow, and hydrogeochemical evolution in a complex volcanic aquifer system, central Ethiopia. *Hydrogeol J* 15:1169–1181
- Deyassa G, Kebede S, Ayenew T, Kidane T (2014) Crystalline basement aquifers of Ethiopia: Their genesis, classification, and aquifer properties. *J Afr Earth Sci* 100(2014):191–202
- Furlong BV, Riley MS, Herbert AW, Ingram JA, Mackay R, Tellam JH (2011) Using regional groundwater flow models for prediction of regional well water quality distributions. *J Hydrol* 398(1–2):1–16
- Gat JR (2010) Isotope hydrology: a study of water cycle. Imperial College, London
- Gamachu D (1977) Aspects of climate and water budget in Ethiopia. Addis Ababa University Press, Addis Ababa
- Glynn PD, Plummer LN (2005) Geochemistry and the understanding of ground-water systems. *Hydrogeol J* 13:263–287
- Güler C, Thyne GD, McCray JE, Turner AK (2002) Evaluation of graphical and multivariate statistical methods for classification of water chemistry data. *Hydrogeol J* 10:455–475
- Hamrla M (1977) The Adola gold field, Ethiopia: geology and genetic hypothesis. *Geologija* 20:247–282
- Heath RC (1983) Basic groundwater hydrology. USGS water supply paper 220
<http://www.iaea.org/water>. Accessed on 04 December 2013
- Hunegnaw A, Sage L, Gonnard R (1998) Hydrocarbon potential of the intracratonic Ogaden Basin, Southeast Ethiopia. *J Pet Geol* 21(4):40–425
- Kebede S (2013) Groundwater in Ethiopia: features, numbers, and opportunities. Springer, Berlin
- Kebede S, Travi Y, Alemayehu T, Ayenew T (2005) Groundwater recharge, circulation and geochemical evolution in the source region of the Blue Nile River, Ethiopia. *Appl Geochem* 20(2005):1658–1676
- Kebede S, Travi Y, Asrat A, Alemayehu T, Ayenew T, Tessema Z (2007) Groundwater origin and flow along selected transects in Ethiopian rift volcanic aquifers. *Hydrogeol J*. doi:10.1007/s10040-007-0210-0
- Kozyrev V, Kebede G, Safonov J, Tullankin V, Woldemichael B (1982) Geological map of the Adola area. Institute of Geological Survey of Ethiopia, Addis Ababa
- Kroner A, Stern RJ (2004) Pan-African Orogeny. *Encycl Geol* 1:1–12
- Leibundgut C, Maloszewski P, Kullis C (2009) Tracers in hydrology. Wiley, Atrium
- Mohr P, Zanettin B (1988) The Ethiopian flood basalt province. *Continental Flood Basalts*. Kluwer Academic Publishers, London, pp 63–110
- MoWIE (2007) Genale-Dawa river basin integrated resources development master plan. Ministry of Water Resources and Energy, Addis Ababa
- Ophori DU, Toth J (1989) Patterns of groundwater chemistry, Ross Creek Basin, Alberta, Canada. *Groundwater* 27(1):20–26
- Piper AM (1944) A graphic procedure in the geochemical interpretation of water analysis. *Trans Am Geophys Union* 25:914–923
- StatSoft Inc (2007) Statistica (Data analysis software system), Version 8.0. www.statsoft.com
- Todd DK, Mays LW (2004) Groundwater hydrology. Wiley, Hoboken
- Toth J (1984) The role of regional gravity flow in the chemical and thermal evolution of groundwater. First Canadian/American conference on Hydrogeology, Banff, Alberta. *Memoir No. 8*
- Tóth J (1963) A theoretical analysis of groundwater flow in small drainage basins. *J Geophys Res* 68:298–315
- Walton NRG (1989) Electrical conductivity and total dissolved solids—What is their precise relationship? *Desalination* 72(3):275–292. doi:10.1016/0011-9164(89)80012-8
- Waterloo Hydrogeologic Inc (2003) AquaChem (Chemical Analysis Software), version 4.0.284. <http://www.waterloohydrogeologic.com>

- Woldehaimanot B, Behrmann JH (1995) A study of metabasite and metagranite chemistry in the Adola region (south Ethiopia): implications for the evolution of the East African Orogeny. *J Afr Earth Sci* 21(3):459–476
- Worku H (1996) Geodynamic development of the Adola Belt (southern Ethiopia) in the Neoproterozoic and its control on gold mineralization. Ph.D. Dissertation, Berlin Technical University
- Worku H, Schandelmeier H (1996) Tectonic evolution of the Neoproterozoic Adola Belt of southern Ethiopia: evidence for Wilson Cycle process and implications for oblique plate collision. *Precambr Res* 77:179–210
- Yibas B, Reimold WU, Armstrong R, Koeberl C, Anhaeusser CR, Phillips D (2002) The tectonostratigraphy, granitoid geochronology and geological evolution of the Precambrian of southern Ethiopia. *J Afr Earth Sci* 34(2002):57–84
- Zewdie G, Nahusenay B (2011) Hydrogeological and hydrochemical mapping of Sede map sheet (NB 37-16). Institute of Geological Survey of Ethiopia, Addis Ababa
- Zewdie G, Sima J (2011) Explanatory notes to hydrogeology and hydrochemical maps of Negele sheet, NB 37-11. AQUATEST, Prague
- Zhou Y, Li W (2011) A review of regional groundwater flow modeling. *Geosci Front* 2(2):205–214
- Zouari K, Trabelsi R, Chkir N (2011) Using geochemical indicators to investigate groundwater mixing and residence time in the aquifer system of Djeffara of Medenine (southeastern Tunisia). *Hydrogeol J* 19:209–219